Crystal and Molecular Structures of Tetrathia[7]heterohelicene: Racemate and Enantiomer

Hiroko Nakagawa, Atsuo Obata, Koh-ichi Yamada, and Hiroshi Kawazura *
Faculty of Pharmaceutical Sciences, Josai University, Sakado, Saitama 350-02, Japan
Michiko Konno
Institute for Solid State Physics, University of Tokyo, Minato-ku, Tokyo 106, Japan
Hiroshi Miyamae
Faculty of Science, Josai University, Sakado, Saitama 350-02, Japan

The crystal and molecular structures of the racemate and enantiomer tetrathia[7]heterohelicene have been determined in order to elucidate their molecular geometries and crystal packing modes. The racemate and enantiomer both crystallize from benzene in the orthorhombic form with $Z = 4$. The former belongs to the space group *Pbcn* with $a = 15.383(2)$, $b = 14.195(2)$, $c = 7.767(1)$ Å, and the latter belongs to the space group $P2_12_12_1$ with $a = 16.975(2)$, $b = 11.236(1)$, $c = 9.186(1)$ Å. The racemate molecule retains C_2 symmetry in the crystal, while the enantiomer lacks this symmetry, primarily because of differences in the dihedral angles between the successive aromatic rings. In the racemate, the molecules are stacked in a column with alternating chirality, while in the enantiomer the molecules are confined orthogonally to each other, resulting in strain. These packing modes are consistent with the observed geometrical deformation of the enantiomer, and provide a clue to the problem of chirality recognition.

A crystal structure survey of carbohelicenes indicates that almost all carbohelicenes ([4]-, [6]-, [7]-, [10]-, and [11]-carbohelicene) in the racemic state are capable of crystallizing in a chiral space group ($P2_12_12_1$ or $P2_1$) except for [5]carbohelicene, for which no chiral habit has been found.[1] This tendency for homochiral aggregation, implying a potential for spontaneous resolution,† is an interesting problem from the viewpoint of chirality recognition, including parity violation, in helical molecules.[4] Is this homochiral aggregation an inherent characteristic of this kind of helical entity? If so, what is its origin? In order to solve this problem, thorough investigation of these helical molecules is a requisite. Indeed, a few carbohelicene homologues with some substituents have been studied[5] to determine whether or not chiral crystals can be obtained from the racemic state, but insufficient data are available for any general conclusion.

Thus, it is of interest to know how other series of helicenes crystallize, *e.g.* thiaheterohelicenes, which we have prepared as a series of homologues[6] composed of alternate thiophene and benzene rings. We have already studied the crystal structure[7] of trithia[5]heterohelicene, the lowest homologue, for which enantiomer resolution was not achieved. However, owing to the transannular interaction between both terminals of the molecule, molecular 'handedness' could be expected. Indeed, the crystal has been found to have, as expected, essentially rigid *P* and *M* enantiomers, which are stacked alternately along the *c*-axis prescribed by the achiral space group *P*2/*c*.

This alternate stacking of heterochiral molecules, evidently different from homochiral aggregation in carbohelicenes, raises several questions. Could the thiaheterohelicenes inherently pile up unlike antipodes alternately? If so, how do like antipodes crystallize? What are the factors involved in chirality recognition? In order to elucidate these problems, we have carried out *X*-ray structure analyses of the racemate and enantiomer of tetrathia[7]heterohelicene. The results are reported here, and the differences between the racemate and enantiomer crystals are discussed.

Experimental

Samples of racemic and enantiomeric (−)-tetrathia[7]heterohelicene were prepared according to the method described previously.[6,8] Both samples were recrystallized from benzene to give pale yellow needles in the case of the racemate and columns in the case of the enantiomer. The crystals employed for data collection had dimensions of *ca.* 0.7 × 0.2 × 0.2 mm for the racemate and 0.3 × 0.3 × 0.3 mm for the enantiomer. Intensity data were collected on a Rigaku AFC-5 four-circle diffractometer, and all the calculations were carried out on a FACOM M-160F computer at this university by the use of the UNICS III[9] and ORTEP II[10] programs. The density was measured by the flotation method.

Crystal Data.—$C_{22}H_{10}S_4$, $M = 402.58$, $F(000) = 824$, orthorhombic, $Z = 4$.

(i) Racemate: $a = 15.383(2)$, $b = 14.195(2)$, $c = 7.767(1)$ Å, $U = 1\,696.0(3)$ Å^3, $D_m = 1.55$, $D_c = 1.58$ g cm^{-3}, Cu-K_α radiation ($\lambda = 1.541\,73$ Å), μ(Cu-K_α) = 50.9 cm^{-1}, and space group *Pbcn*.

(ii) Enantiomer: $a = 16.975(2)$, $b = 11.236(1)$, $c = 9.186(1)$ Å, $U = 1\,752.2(4)$ Å^3, $D_m = 1.53$, $D_c = 1.53$ g cm^{-3}, Mo-K_α radiation ($\lambda = 0.710\,69$ Å), μ(Mo-K_α) = 5.2 cm^{-1}, and space group $P2_12_12_1$.

Structure Determination.—A total of 1 694 reflections in the range $2\theta < 130°$ ($h, k, l \geqq 0$), and 4 603 for $2\theta < 70°$ ($h, k, l \geqq 0$) were collected by the 2θ–ω scan technique for the racemate and the enantiomer, respectively. During data collection, three standard reflections were monitored every 50 reflections, and they showed no significant variations in their intensities. The unit-cell parameters were refined from least-squares fits of 22 reflections ($57 < 2\theta < 67$) for the racemate and 25 reflections ($26 < 2\theta < 35$) for the enantiomer. Finally, 1 227 reflections having $|F_o| < 2\sigma(|F_o|)$ were used for the structure determination of the racemate and 2 145 having $|F_o| < 3\sigma(|F_o|)$ for that of the enantiomer. Each data set was

---

† In hexahelicene, spontaneous resolution is hampered by a phenomenon which has recently been described as 'lamellar twinning'[2] or 'enantiomeric intergrowth',[3] but this phenomenon itself implies the capability for chirality recognition.

Table 1. Determination of absolute configuration

h	*k*	*l*	ΔF_c†	ΔF_o‡	*h*	*k*	*l*	ΔF_c†	ΔF_o‡
3	1	1	−5.15	−2.55	8	2	1	−4.25	−3.14
1	0	2	8.60	2.26	2	2	2	−3.46	−2.07
5	2	2	−6.27	−2.23	0	1	3	3.97	4.54
0	2	3	2.33	2.50	1	3	3	5.14	3.20
2	0	4	3.54	2.36	1	1	4	5.06	2.12
3	2	4	3.90	2.28	10	3	1	−4.95	−5.75
5	6	1	5.39	3.66	1	8	1	11.01	7.46
8	2	2	−3.02	−2.44	7	5	2	5.56	3.57
4	6	2	5.30	2.99	1	7	2	6.37	2.61
6	6	3	10.49	6.43	3	7	3	8.16	6.95
3	4	4	5.90	3.04	5	5	4	10.16	5.26
0	3	5	5.22	11.02	4	4	5	6.92	3.77

† $\Delta F_c = |F_c(hkl)| - |F_c(hk\bar{l})|$. ‡ $\Delta F_o = |F_o(hkl)| - |F_o(hk\bar{l})|$.

corrected for Lorentz and polarization effects, but not for absorption. The structures were solved by the heavy-atom and Fourier methods, and refined by the block-diagonal least-squares approximation; $\Sigma w(|F_o| - |F_c|)^2$ was minimized with $w = 1.0$. The hydrogen atoms were located from difference-Fourier syntheses. Complex neutral-atom scattering factors were taken from ref. 11. The final R $\{= \Sigma(|F_o| - |F_c|)/\Sigma|F_o|\}$ values were 0.048 and 0.045, and the R_w $(= \{\Sigma w(|F_o| - |F_c|)^2/w|F_o|^2\}^{0.5})$ values were 0.050 and 0.044 for the racemate and the enantiomer, respectively. The $(\Delta/\sigma)_{\text{max.}}$ values were 0.032 and 0.186 and the maximum heights in the final difference Fourier synthesis were 0.30 and 0.29 e Å^{-3} for the racemate and the enantiomer, respectively.

Determination of the Absolute Configuration.—Final refinements were perfomed by an anomalous scattering technique. Cu-K_α radiation was used to measure Bijvoet pairs of 295 reflections among which 24 pairs with the larger value of $\{|F_c(hkl)| - |F_c(hk\bar{l})|\}/\sigma F_o(hkl)$ [$\sigma F_o(hkl)$, is the standard deviation of $F_o(hkl)$] are collected in Table 1. The concordance of the signs of $\Delta|F_o|$ and $\Delta|F_c|$ indicates that the absolute crystal structure listed in Table 2 is correct. This result confirmed that (−)-thiaheterohelicene has an *M*-configuration, and this is the same as in the case of carbohelicenes.[12]

The final atomic parameters with estimated standard deviations are listed in Table 2 for the racemate and enantiomer crystals. The atom-numbering scheme, and the nomenclature of the rings, are shown in Figure 1. Observed and calculated structure factors, thermal parameters of the atoms, full bond lengths and angles, and data on least-squares planes are tabulated in Supplementary Publication No. SUP 56366 (31 pp.).*

Discussion

Molecular Geometry.—As regards bond lengths,† both molecules tend to have shorter outer core bonds and longer inner core bonds, as observed in carbohelicene[1] and also in trithia[5]heterohelicene[5] (Table 3).

The planarity of the aromatic rings in the molecules is apparent from the mean deviations of the atoms from the least-squares plane of the ring (Table 4). In both molecules, the terminal rings A and A′ have an almost flat configuration, but the planarity is poorer towards the middle rings and is poorest in the central D ring. The increase of configurational deformation towards the middle rings correlates well with the variation in the dihedral angle between adjacent rings (Table 5), *i.e.* the increase of the angle towards the middle part of the helix. These configurational changes, however, are common to the racemate and enantiomer.

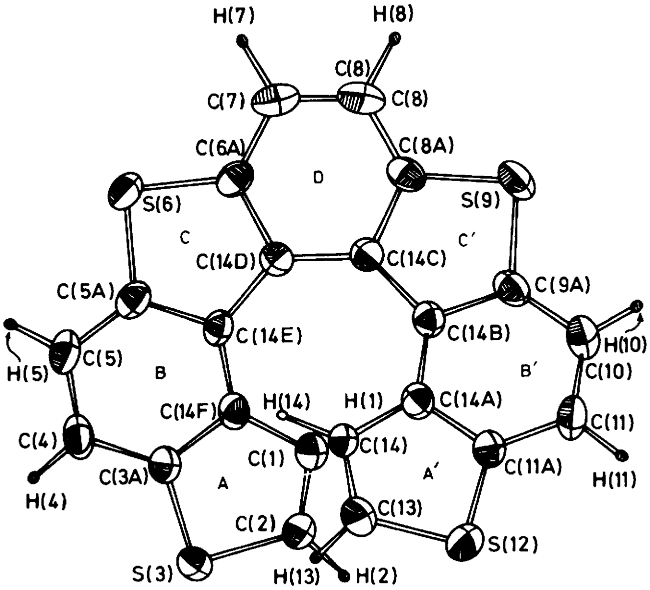

Figure 1. Schematic drawing of the molecule showing the atom numbering and the ring-labelling scheme

A noteworthy feature is the loss of C_2 symmetry in the enantiomer. This asymmetric deformation is clearly apparent in the dihedral angles (Table 5), which show an especially marked disparity in the cases of B–C and B′–C′. As a result of this asymmetric deformation, the enantiomer has a smaller aperture between its two terminal thiophene rings than the racemate molecule, as reflected by the dihedral angles A–A′. This means that the enantiomer is more crushed along the helical axis than the racemate.

Correspondingly, significant shortenings of the non-bonded carbon–carbon distances in the enantiomer are seen between the carbons located at the frontier of the opposed terminal thiophene rings, *i.e.*, C(1)–C(14) and C(2)–C(13), and hence C(1)–C(13) and C(2)–C(14) (Table 6). However, the non-bonded carbon–carbon distances other than above are rather lengthened in the enantiomer. This may be caused by the increase of the internal angle C(14)–C(14A)–C(14B) in the

---

* For details of Supplementary Publications see Instructions for Authors in *J. Chem. Soc., Perkin Trans. 2*, 1985, Issue 1.

† In the enantiomer molecule, an apparent contraction of the C(8)–C(7) bond was observed owing to excessive thermal motion of C(8) (see SUP) but its magnitude did not exceed the standard deviation.

Table 2. Atomic co-ordinates ($\times 10^4$ for non-hydrogen atoms and $\times 10^3$ for hydrogen atoms)*

(i) Racemate

	x	y	z
S(3)	1 117(1)	4 021(1)	5 591(2)
S(6)	1 956(1)	−46(1)	3 396(2)
C(1)	−19(3)	2 847(3)	4 439(5)
C(2)	59(3)	3 710(3)	5 183(6)
C(3A)	1 487(3)	2 950(3)	4 802(6)
C(4)	2 348(3)	2 628(3)	4 916(6)
C(5)	2 519(3)	1 710(3)	4 457(6)
C(5A)	1 848(3)	1 154(3)	3 802(6)
C(6A)	859(3)	−137(3)	2 887(5)
C(7)	435(3)	−1 001(3)	2 635(6)
C(14D)	440(3)	745(3)	2 822(5)
C(14E)	996(2)	1 479(3)	3 523(5)
C(14F)	800(2)	2 396(3)	4 170(5)
H(1)	−59(3)	257(3)	416(5)
H(2)	−42(3)	418(3)	549(5)
H(4)	279(3)	305(3)	546(5)
H(5)	306(3)	139(3)	456(5)
H(7)	78(3)	−164(3)	268(6)

(ii) Enantiomer

	x	y	z
S(3)	3 870(1)	4 305(1)	1 005(2)
S(6)	499(1)	2 400(1)	1 805(2)
S(9)	−368(1)	7 106(1)	−1 262(2)
S(12)	2 424(1)	8 988(1)	2 338(2)
C(1)	2 638(3)	5 392(4)	80(5)
C(2)	3 431(3)	5 444(4)	48(5)
C(3A)	2 960(3)	3 712(4)	1 445(5)
C(4)	2 841(3)	2 624(4)	2 165(5)
C(5)	2 092(3)	2 223(4)	2 344(6)
C(5A)	1 468(3)	2 904(4)	1 812(5)
C(6A)	198(3)	3 692(4)	948(6)
C(7)	−563(3)	3 827(5)	380(7)
C(8)	−728(3)	4 829(6)	−375(7)
C(8A)	−188(3)	5 743(5)	−433(6)
C(9A)	480(3)	7 705(4)	−501(5)
C(10)	686(3)	8 911(5)	−621(6)
C(11)	1 303(3)	9 339(4)	156(6)
C(11A)	1 693(3)	8 581(4)	1 111(5)
C(13)	2 438(3)	7 587(4)	3 070(5)
C(14)	1 931(3)	6 840(4)	2 439(5)
C(14A)	1 496(3)	7 361(4)	1 267(5)
C(14B)	898(2)	6 890(4)	352(5)
C(14C)	551(3)	5 700(4)	275(5)
C(14D)	790(2)	4 551(4)	796(5)
C(14E)	1 551(2)	4 041(4)	1 187(5)
C(14F)	2 341(2)	4 415(3)	915(4)
H(1)	231(2)	594(3)	−34(4)
H(2)	374(3)	598(5)	−33(6)
H(4)	323(2)	221(4)	251(5)
H(5)	198(2)	149(4)	271(5)
H(7)	−97(3)	328(4)	42(6)
H(8)	−119(3)	494(4)	−74(5)
H(10)	41(3)	942(4)	−111(5)
H(11)	142(3)	1 014(4)	15(5)
H(13)	277(2)	747(4)	382(5)
H(14)	187(2)	608(4)	276(4)

* For atom numbering, see Figure 1.

enantiomer [130.3(4)° in the racemate and 131.4(4)° in the enantiomer], and this increase is probably due to the reduction of the dihedral angles A–B and B–C in the enantiomer molecule (see Table 5). Thus, the enantiomer molecule is slightly spread vertically to the helical axis instead of having a crushed configuration.

Table 3. Selected bond lengths (Å)*

	Racemate	Enantiomer
C(4)–C(5)	1.376(7)	1.359(8)
C(10)–C(11)	1.376(7)	1.356(8)
C(7)–C(8)	1.356(7)	1.351(9)
mean (outer)	1.368(7)	1.355(8)
C(14E)–C(14F)	1.426(5)	1.428(6)
C(14A)–C(14B)	1.426(5)	1.420(6)
C(14C)–C(14D)	1.443(6)	1.435(6)
mean (inner)	1.432(5)	1.428(6)

* For atom numbering, see Figure 1.

Table 4. Mean deviations (Å) of the ring atoms from the least-squares planes of the rings*

Ring	Racemate	Enantiomer
A	0.013(3)	0.013(3)
A′	0.013(3)	0.009(3)
B	0.030(3)	0.022(3)
B′	0.030(3)	0.026(4)
C	0.035(3)	0.031(3)
C′	0.035(3)	0.034(3)
D	0.055(3)	0.061(4)

* For ring labelling, see Figure 1.

Table 5. Selected dihedral angles (°) between the least-squares planes of the rings*

Ring–ring	Racemate	Enantiomer
A–B	8.8(2)	6.4(2)
A′–B′	8.8(2)	6.7(2)
B–C	8.6(1)	7.3(1)
B′–C′	8.6(1)	9.0(2)
C–D	11.3(1)	11.6(2)
C′–D′	11.3(1)	12.4(2)
A–A′	48.6(1)	45.9(1)

* For ring labelling, see Figure 1.

Table 6. Selected non-bonded atom–atom distances between the terminal thiophene rings (Å)*

	Racemate	Enantiomer
C(1)–C(14)	3.012(6)	2.963(6)
C(1)–C(14A)	3.116(6)	3.137(6)
C(14)–C(14F)	3.116(6)	3.141(6)
C(1)–C(14B)	3.364(6)	3.408(6)
C(14)–C(14E)	3.364(6)	3.410(6)
C(1)–C(13)	3.794(6)	3.707(6)
C(14)–C(2)	3.794(6)	3.710(7)
C(2)–C(13)	4.171(7)	4.043(7)
C(1)–H(14)	2.97(4)	2.89(4)
C(14)–H(1)	2.97(4)	2.82(4)
C(14A)–H(1)	2.62(4)	2.58(4)
C(14F)–H(14)	2.62(4)	2.64(4)
H(1)–H(14)	3.15(6)	2.94(6)

* For atom numbering, see Figure 1.

The non-bonded distances of the terminal hydrogen atoms to the ring carbon atoms are larger than the van der Waals' contact distances in both molecules (Table 6), and thus in the enantiomer these non-bonded distances simply reflect the skeletal deformation.

Packing Mode.—The racemate crystallizes in achiral space group *Pbcn* with $Z = 4$. The structure is shown in Figure 2, as a projection along the c-axis. The crystal symmetry affords an

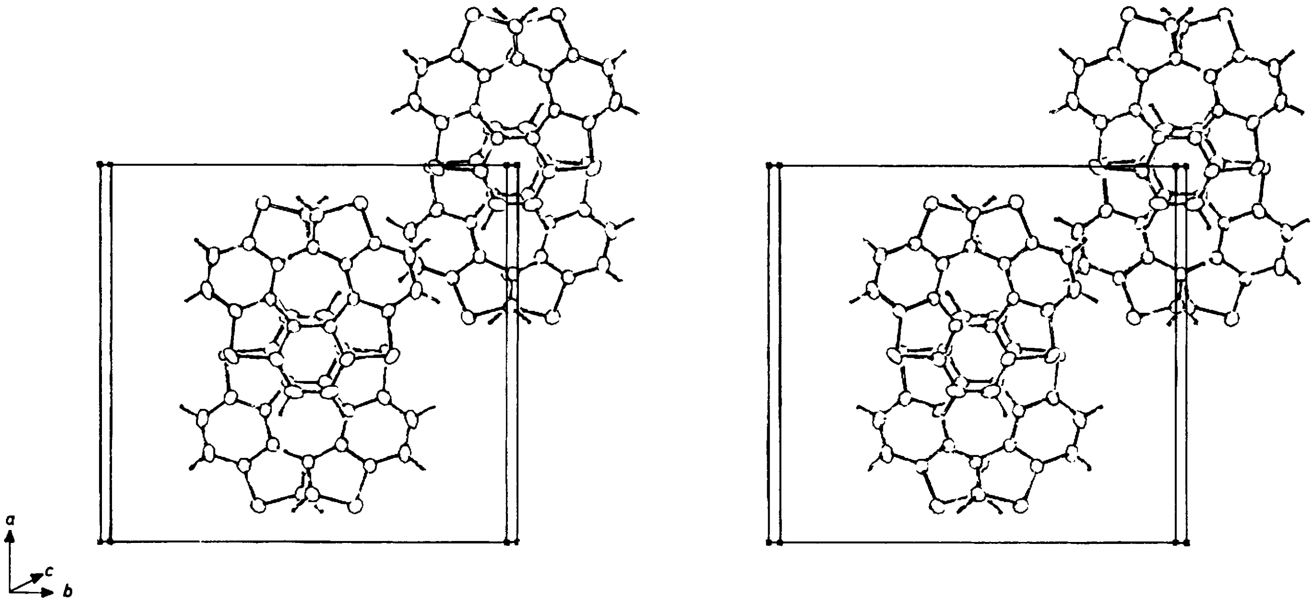

Figure 2. Projection of the racemate along the *c*-axis

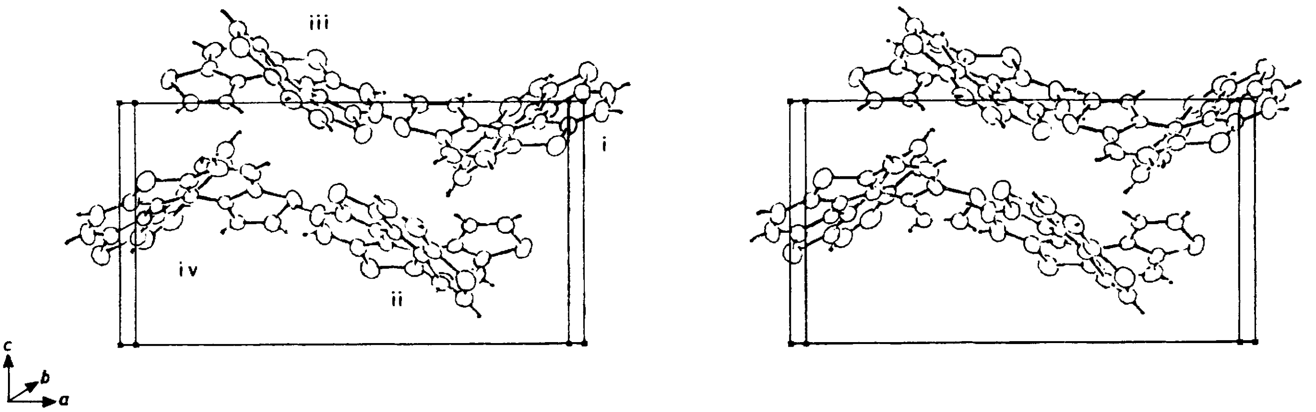

Figure 3. Projection of the enantiomer along the *b*-axis

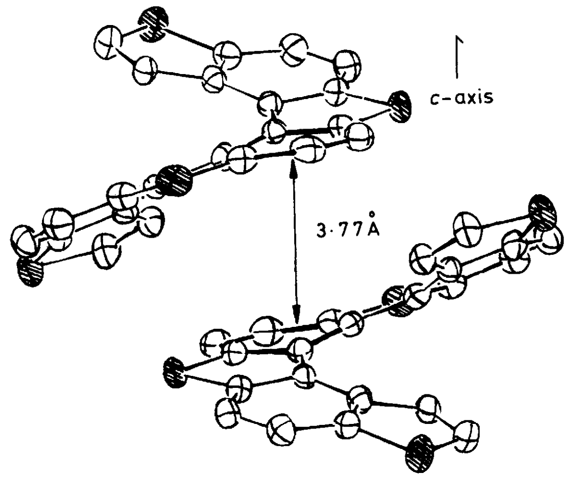

Figure 4. A perspective drawing of the stacked molecules in the racemate

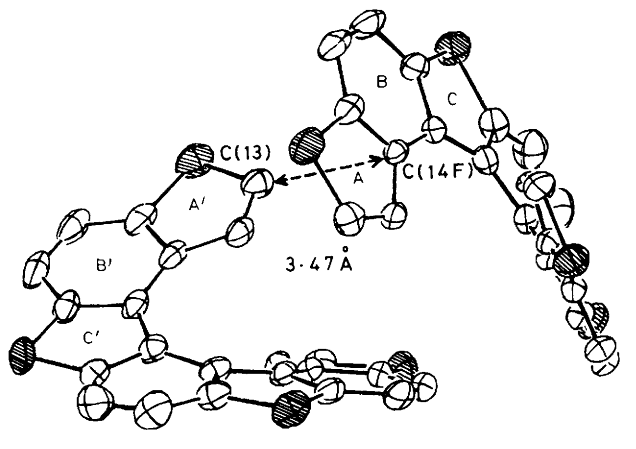

Figure 5. Orthogonal packing of the enantiomer

alternate stacking of *P* and *M* molecules along the *c*-axis so as to overlap the central benzene rings (D-rings). However, avoidance of direct overlap of the π-electron clouds between the rings is attained not by an elongation of the interplanar distance, but by a slipping of the rings, which is manifested by an appreciable tilt of the rings from the *ab* plane [13.9(1)° for both *P* and *M* molecules]. Thus, the mean interplanar distance between them remains at 3.77 Å, which is not suggestive of any strong intermolecular interaction. The features of the system are shown in Figure 4.

This stacking feature of racemic thia[7]heterohelicene resembles that of the thia[5]heterohelicene crystal, in which alternately stacked *P* and *M* molecules overlap their central thiophene rings with a separation of 3.5 Å. Thus, it seems feasible that in the racemic thiaheterohelicenes (at least the lower homologues) there is a tendency for alternate stacking of the unlike antipodes, irrespective of the overlapping moieties, *i.e.* thiophene or benzene ring.

The entantiomer molecules crystallize, of course, in chiral space group $P2_12_12_1$ with $Z = 4$. The packing features are shown in Figure 3 as a projection along the *b*-axis. Four molecules in the lattice are designated according to their symmetry operations as i (x, y, z), ii $(0.5 - x, 1 - y, 0.5 + z)$, iii $(0.5 + x, 1.5 - y, - z)$, and iv $(1 - x, 0.5 + y, 0.5 - z)$. No stacking or overlapping between the molecules was found, but there is an orthogonal approach of the terminal thiophene ring of one molecule to the terminal moiety of the nearest neighbour molecule (molecule i to ii and molecule iv to iii in Figure 3).

An illustration of the above situation is shown in Figure 5. The terminal A′ ring of molecule i makes dihedral angles of 67.1(2)° and 64.5(2)° and 67.1(2)° with rings A and B and C of molecule ii, respectively, and C(13) of molecule i approaches C(14F) of molecule ii at the distance of 3.47(6) Å, which might have a substantial influence on the geometry of molecule ii. Indeed, the asymmetric geometry of the enantiomer already described can be well understood in terms of this nearly orthogonal approach.

As is clear from Figure 5, compression of the terminal group of molecule i and the terminal moiety of molecule ii may cause a decrease of the dihedral angle B–C. This is in agreement with the observed geometry of the enantiomer molecule (Table 5).

The enantiomer molecules do crystallize in the space group that allows the closest packing,[4] but at the expense of some geometrical deformation. This crystallization habit may be the reason why the racemic thiahelicenes do not give a crystal with a chiral space group, unlike the carbohelicenes.

Now we may discuss the question of chirality recognition. Evidently, the phenomenon of alternate heterochiral aggregation, as well as that of homochiral aggregation, is a result of the chiral recognition of each antipode. We may say that the thiahelicenes (at least the lower homologues) prefer to stack the unlike antipode because the aggregation of the like antipode requires geometrical deformation. We have already established that chiral discrimination of tetrathial[7]heterohelicene through diastereomeric interactions depends on the geometrical disparity of the diastereoisomers.[13] Thus, it seems reasonable that enantiomer discrimination also occurs through geometrical perturbation of the molecules involved.

A thorough investigation of the crystal habits of helicene families may well provide further interesting results on chirality discrimination.

References

1 R. Kuroda, *J. Chem. Soc., Perkin Trans. 2*, 1982, 789.
2 B. S. Green and M. Knosson, *Science*, 1981, **214**, 795.
3 S. Ramdas, J. M. Thomas, M. E. Jordan, and C. J. Eckhardt, *J. Phys. Chem.*, 1981, **85**, 2421.
4 S. F. Mason, *Int. Rev. Phys. Chem.*, 1983, **3**, 217.
5 G. W. Frank, D. T. Hefelfinger, and D. A. Lighter, *Acta Crystallogr.*, 1973, **B29**, 223; Th. E. M. Van der Hark and J. H. Noordik, *Cryst. Struct. Commun.*, 1973, **2**, 643; Th. E. M. Van der Hark, J. H. Noordik, and P. T. Beurskens, *ibid.*, 1974, **3**, 443; J. P. Declercq, G. Germain, M. Van Meerssche, and T. Debaerdemaeker, *Acta Crystallogr.*, 1976, **B32**, 335; S. S. Wijmenga, H. Numan, and A. Vos, *ibid.*, 1978, **B34**, 846; W. Marsh and J. D. Dunitz, *Bull. Soc. Chim. Belq.*, 1979, **88**, 847; H. M. Doesburs, *Cryst. Struct. Commun.*, 1980, **9**, 137.
6 K. Yamada, S. Ogashiwa, H. Tanaka, H. Nakagawa, and H. Kawazura, *Chem. Lett.*, 1981, 343.
7 H. Nakagawa, K. Yamada, H. Kawazura, and H. Miyamae, *Acta Crystallogr.*, 1984, **C40**.
8 H. Nakagawa, S. Ogashiwa, H. Tanaka, K. Yamada, and H. Kawazura, *Bull. Chem. Soc. Jpn.*, 1981, **54**, 1903.
9 T. Sakurai and K. Kobayashi, *Rikagaku Kenkyusho Hokoku*, 1978, **55**, 69.
10 C. K. Johnson, ORTEP II, Report ORNL-5138, Oak Ridge National Laboratory, Oak Ridge, 1976.
11 'International Tables for *X*-Ray Crystallography,' Kynoch Press, Birmingham, 1974, vol. IV.
12 D. A. Lightner, D. T. Hefelfinger, T. W. Powers, G. W. Frank, and K. N. Trueblood, *J. Am. Chem. Soc.*, 1972, **94**, 3492.
13 H. Nakagawa, H. Tanaka, K. Yamada, and H. Kawazura, *J. Phys. Chem.*, 1982, **86**, 2311.

Received 19*th November* 1984; *Paper* 4/1957